

Simultaneous efficiency enhancement and self-cleaning effect of white organic light-emitting devices by flexible antireflective films

Dong Wu,¹ Yong-Biao Zhao,² Si-Zhu Wu,¹ Yue-Feng Liu,¹ Hao Zhang,¹ Shuai Zhao,¹ Jing Feng,¹ Qi-Dai Chen,¹ Dong-Ge Ma,^{2,4} and Hong-Bo Sun^{1,3,5}

¹State Key Laboratory on Integrated Optoelectronics, College of Electronic Science and Engineering, Jilin University, 2699 Qianjin Street, Changchun 130023, China

²State Key Laboratory of Polymer Physics and Chemistry, Changchun Institute of Applied Chemistry, Chinese Academy of Sciences, Changchun 130022, China

³College of Physics, Jilin University, 119 Jiefang Road, Changchun 130023, China

⁴e-mail: mdg1014@ciac.jl.cn

⁵e-mail: hbsun@jlu.edu.cn

Received April 21, 2011; revised June 12, 2011; accepted June 14, 2011;
posted June 14, 2011 (Doc. ID 146214); published July 12, 2011

In this Letter, we report the improved light outcoupling efficiency of conventional white organic light-emitting devices (OLEDs) by a kind of multifunctional film with both antireflective and superhydrophobic ability. This film consisted of regular polydimethylsiloxane (PDMS) nanopillar arrays, which were readily batch produced by low-cost imprint lithography. The nanopillar arrays could effectively eliminate the light total reflection and enhance the device efficiency of OLEDs by producing the gradual refractive index due to the decreasing material density from glass to air. Moreover, owing to its superhydrophobicity (contact angle $\sim 151^\circ$), the antireflective film exhibited self-cleaning ability, which was beneficial for keeping the OLEDs substrate clean and ensure the high efficiency of OLEDs. This method is simple, cost-effective, and reproducible. The OLEDs showed an efficiency enhancement of 25% with the multifunctional film. © 2011 Optical Society of America

OCIS codes: 090.2880, 230.3670, 310.1210, 310.6628.

White organic light-emitting devices (OLEDs) exhibited many desirable features, such as ultrathin, light weight, and good flexibility, and thus have been considered as a new generation of solid-state lighting sources [1–3]. However, a shortcoming of conventional bottom-emitting OLEDs fabricated on a flat glass substrate is that only a small fraction (<20%) of the light generated in the device can escape with the 80% trapped in the glass substrate (glass mode) and the high index organic layer (waveguided modes). Many techniques have been developed to enhance the outcoupling efficiency. To outcouple the waveguided light, methods such as textured microstructures [4], surface plasmons [5–7], microcavities [8,9], and low refractive index silica aerogel layer [10], have been adopted. On the other hand, to extract the glass-mode light, methods, such as microlens arrays with different geometries [11,12] and the high refractive index substrate [13], have been developed. However, some of the reported methods have distorted or shifted emission spectrum, or complicated fabrication process. Alternatively, Li [14] *et al.* demonstrated a simple method—using antireflective surfaces to extract the glass-mode light of white OLEDs without spectral distortion. The antireflective silica cone arrays were directly prepared on the opposite side of fused silica substrate by nanosphere lithography and reactive ion etching (RIE), but this method was confined to the fused silica substrate. As we know, the most common substrate of OLEDs is a kind of amorphous material—glass, which was difficult etch by RIE.

Imprint lithography [15] is a simple, cost-effective, and high through method for functional microstructures. In this Letter, we reported the improved light outcoupling

efficiency of conventional OLEDs by antireflective nanopillar arrays prepared by low-cost imprint lithography. The light loss of the total reflection at the glass substrate and air interface was effectively lowered owing to the gradient refractive index. The antireflective film was found possessing self-cleaning superhydrophobic ability, exhibiting a high contact angle (CA) (151°). This is beneficial to prevent the OLEDs from being polluted by dust particles in practical applications.

Shown in Figs. 1(a) and 1(b) are the reference bottom-emitting OLEDs structure (Glass/ITO(120 nm)/M(30 nm)/NPB(20 nm)/BePP₂(5 nm)/CBP(3 nm)/CBP:Ir(PPy)₃(10 nm)/Bphen(20 nm)/Alq₃(20 nm)/LiF(1 nm)/Al(100 nm)) and the OLEDs with antireflective films. The material M is 4, 4', 4''-tris(3-methylphenylphenylamino)triphenylamine (*m*-MTDATA) which is a kind of hole injection materials. The N, N'-diphenyl-N, N'-bis(1, 1'-biphenyl)-4, 4'-diamine (NPB) was used as the hole transporting layer and the tris-(8-hydroxyquinoline) aluminum (Alq₃) was the electron transporting layer. Three emitting layers composed of bis 4, 4'-Bis(carbazol-9-yl)biphenyl: tris[1-phenyl isoquinolinato-C₂, N] iridium(III) (CBP: Ir(Piq)₃), 4, 4'-Bis(carbazol-9-yl)biphenyl: fac tris(2-phenylpyridine) iridium (CBP: Ir(ppy)₃), and bis [2-(2-hydroxyphenyl)pyridine]beryllium (BePP₂) were used to harvest red, green, and blue light, respectively. White light composed of these three kinds of light penetrates the glass substrate and emitting into the air. Owing to the critical angle of the total reflection, when light passes from a high to a low refractive index medium, rays with an internal emission angle greater than the critical angle would be internally reflected. This phenomenon happens at the glass substrate and air interface in the reference

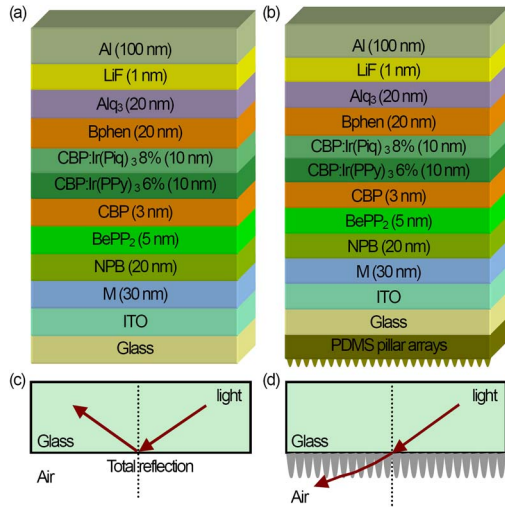


Fig. 1. (Color online) External quantum efficiency enhancement of white OLEDs by antireflective films. (a) and (b) The reference OLEDs structure and the OLEDs with antireflective films. (c) and (d) The light outcoupling mechanism.

device which results in trapped light in the glass substrate. According to the Snell–Descartes law calculation, the critical angle is about 34.8° . To outcouple the emitting light, antireflective film was transferred onto the opposite side of the ITO-coated glass substrate [Fig. 1(b)], because the nanopillar arrays with tapered morphology showed a gradient refractive index and could effectively lower the light loss of the total reflection [Fig. 1(d)] by modifying the critical angle.

Figures 2(c) and 2(d) are the 45° tilted-view scanning electron microscopic (SEM) and locally magnified image of regular nanopillar arrays prepared by soft transfer of the hole arrays [Fig. 2(a)] template [16,17]. Here, the width of the hole was decreased to about the subwavelength magnitude (~ 440 nm) by increasing the interference angle. The height was about 500 nm controlled by the thickness of the SU-8 resin (Nano MicroChem). The hole template was transferred by polydimethylsiloxane (PDMS) Sylgard 184 purchased from Dow Corning (MI) which exhibited good elasticity, high optical transmit-

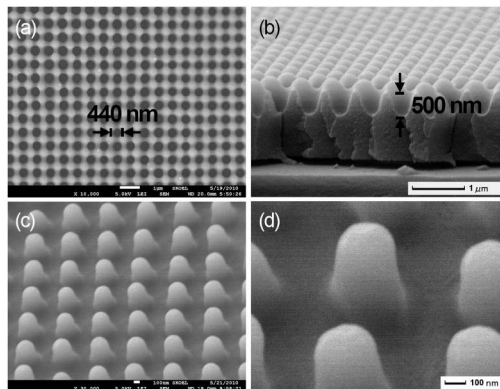


Fig. 2. Antireflective nanopillar arrays prepared by low-cost imprint lithography. (a) Top-view from the SEM of the hole template. (b) Cross-sectional SEM image of the template. (c) and (d) 45° tilted-view of the SEM and locally magnified image of the regular nanopillar arrays.

tance, and biocompatibility. As shown in Figs. 2(c) and 2(d), the nanopillar arrays are uniform, similar to the nipple arrays on the eyes of the moth [18], which suppresses the reflection loss and increases the transmittance of light.

To systematically investigate the optical performance of the nanopillar arrays, the optical transmittance spectra of a flat PDMS film and the film with PDMS nanopillar arrays were measured [Fig. 3(b)]. The pillar arrays exhibit transmittance of about 95% over a spectral range from 400 to 800 nm, while the transmittance of the flat surface is less than 91%. The improved transmittance is attributed to the tapered nanopillar arrays, which produce the gradual refractive index due to the decreasing material density from glass to air. The antireflective film was put onto the opposite side of the glass substrate to output the emitting light of conventional OLEDs. Shown in Fig. 3(a) are the electroluminescent (EL) spectra of the OLEDs with and without antireflective surfaces at the voltage of 11 V in the normal direction. We could find that the EL intensity was significantly enhanced by the antireflective film. There are three main peak wavelengths of 620, 510, 460 nm produced by the three emitters mentioned earlier. It is worth mentioning that the intensity of the whole wavelengths from 400 to 760 nm was significantly improved, which demonstrated that the efficiency enhancement by the antireflective film was not confined to certain wavelengths. Figure 3(c) shows the voltage-luminance characteristics of the OLEDs without and with antireflective films measured in the normal direction. Obviously, the luminance of the OLEDs with the antireflective films is much bigger than the reference one. Moreover, the current efficiencies of the OLEDs with and without antireflective film as a function of the voltage were investigated [Fig. 3(d)]. Compared with the reference OLEDs, the current efficiency for the OLEDs with antireflective film is enhanced by 25%.

Self-cleaning superhydrophobic function is sometimes needed for keeping the high performance of the optical

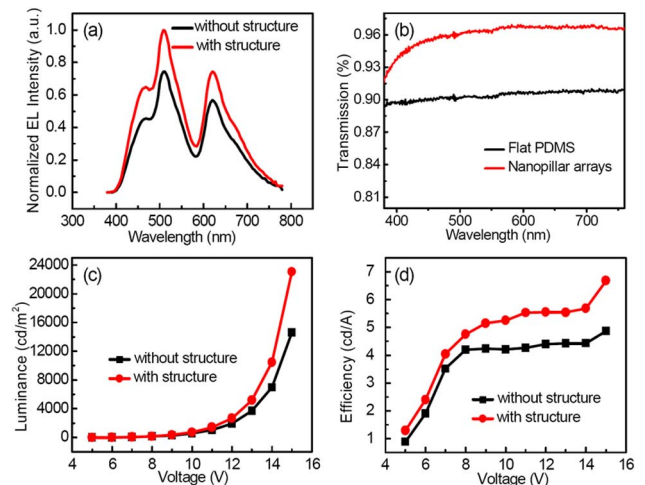


Fig. 3. (Color online) (a) Enhanced EL intensity in the normal direction of the OLEDs by the antireflective films. (b) The optical transmittance spectra of the flat PDMS surface and nanopillar arrays. (c) and (d) Luminance and current efficiency characteristics of the OLEDs with and without antireflective films as a function of current density.

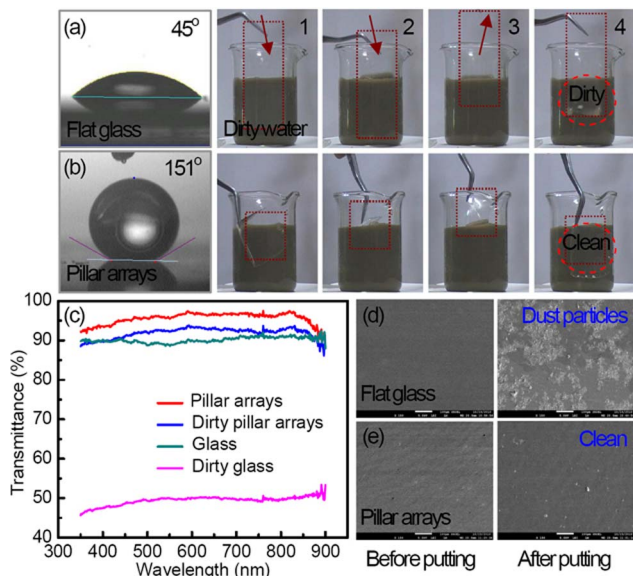


Fig. 4. (Color online) Self-cleaning superhydrophobic ability of the nanopillar arrays. (a) and (b) The wetting property and antidust ability of the flat surface and nanopillar arrays. (c) The optical transmittance before and after being immersed into dirty water. (d) and (e) Comparison of the flat glass and pillar arrays characterized by the SEM image.

devices [19]. Generally, the surface with a CA larger than 150° is defined as a superhydrophobic surface determined by surface micro/nanostructures and low-surface energy [20,21]. Owing to the nanopillar structures and the inherent low-surface energy of PDMS [16], the antireflective film exhibits a high CA (151°) [Fig. 4(b)]. We could find that the surface kept clean even when it was put into dirty water (Media 1). In contrast, the California for the common glass surface was very low (45°), and its surface became dirty after it was immersed into dirty water [Fig. 4(a) and Media 2]. To quantitatively investigate the self-cleaning effect, the optical transmittance of these surfaces was measured [Fig. 4(c)]. For the superhydrophobic nanopillar arrays, the optical transmittance slightly decreased ($<5\%$) after the surface was put into the dirty water, while the transmittance for the flat surface significantly decreased from 90% to 50%. Moreover, both the flat surface and the nanopillar arrays were investigated by the SEM. We found that there were a lot of dust particles on the flat surface, while the nanopillar arrays kept clean. This further demonstrates the self-cleaning ability of the nanopillar arrays.

In conclusion, we have reported a simultaneous efficiency enhancement and a self-cleaning effect of white OLEDs by flexible antireflective films which were

prepared by low-cost imprint lithography. This film consisting of regular nanopillar arrays could effectively lower the light loss of the total reflection and outcouple the emitting light of the OLEDs by producing a gradient refractive index from glass to air. The self-cleaning functions will be beneficial in keeping the high-efficiency of the OLEDs. The simple, cost-effective, and reproducible method may find great applications in the illumination and display.

This work was supported by the National Natural Science Foundation of China (NSFC) under grants 90923037 and 60677016.

References

1. Y. Sun and S. R. Forrest, *Nat. Photon.* **2**, 483 (2008).
2. S. Reineke, F. Lindner, G. Schwartz, N. Seidler, K. Walzer, B. Lüssem, and K. Leo, *Nature* **459**, 234 (2009).
3. B. W. D'Andrade, R. J. Holmes, and S. R. Forrest, *Adv. Mater.* **16**, 624 (2004).
4. I. Schnitzer, E. Yablonovitch, C. Caneau, T. J. Gmitter, and A. Scherer, *Appl. Phys. Lett.* **63**, 2174 (1993).
5. J. Feng, T. Okamoto, and S. Kawata, *Opt. Lett.* **30**, 2302 (2005).
6. C. L. Lin, T. Y. Cho, C. H. Chang, and C. C. Wu, *Appl. Phys. Lett.* **88**, 081114 (2006).
7. C. J. Yates, I. D. W. Samuel, P. L. Burn, S. Wedge, and W. L. Barnes, *Appl. Phys. Lett.* **88**, 161105 (2006).
8. R. H. Jordan, L. J. Rothberg, A. Dodabalapur, and R. E. Slusher, *Appl. Phys. Lett.* **69**, 1997 (1996).
9. J. Grüner, R. Cacialli, and R. H. Friend, *J. Appl. Phys.* **80**, 207 (1996).
10. T. Tsutsui, M. Yahiro, H. Yokogawa, K. Kawano, and M. Yokoyama, *Adv. Mater.* **13**, 1149 (2001).
11. S. Moller and S. R. Forrest, *J. Appl. Phys.* **91**, 3324 (2002).
12. Y. Sun and S. R. Forrest, *J. Appl. Phys.* **100**, 073106 (2006).
13. T. Nakamura, N. Tsutsumi, N. Juni, and H. Fujii, *J. Appl. Phys.* **97**, 054505 (2005).
14. Y. Li, F. Li, J. Zhang, C. Wang, S. Zhu, H. Yu, Z. Wang, and B. Yang, *Appl. Phys. Lett.* **96**, 153305 (2010).
15. C. H. Sun, A. Gonzalez, N. C. Linn, P. Jiang, and B. Jiang, *Appl. Phys. Lett.* **92**, 051107 (2008).
16. D. Wu, S. Z. Wu, Q. D. Chen, Y. L. Zhang, J. Yao, X. Yao, L. G. Niu, J. N. Wang, L. Jiang, and H. B. Sun, *Adv. Mater.* **23**, 545 (2011).
17. D. Wu, Q. D. Chen, B. B. Xu, J. Jiao, Y. Xu, H. Xia, and H. B. Sun, *Appl. Phys. Lett.* **95**, 091902 (2009).
18. A. R. Parker and H. E. Townley, *Nature Nanotechnol.* **2**, 347 (2007).
19. J. Zhu, C. M. Hsu, Z. Yu, S. Fan, and Y. Cui, *Nano Lett.* **10**, 1979 (2010).
20. D. Wu, Q. D. Chen, H. Xia, J. Jiao, B. B. Xu, X. F. Lin, Y. Xu, and H. B. Sun, *Soft Matt.* **6**, 263 (2010).
21. D. Wu, Q. D. Chen, J. Yao, Y. C. Guan, J. N. Wang, L. G. Niu, H. H. Fang, and H. B. Sun, *Appl. Phys. Lett.* **96**, 053704 (2010).